Integrated AIS Collision-Risk Mapping in the Lombok Strait TSS

Nenny[1*], Albertha Lolo Tandung[2], Joe Ronald K. Bokau[3], Adnan[4], and Muh. Arifin[5]
(Received: 10 June 2026 / Revised: 12 June 2026 / Accepted: 17 July 2026 / Available Online: 1 September 2026)

Abstract**—** The Lombok Strait Traffic Separation Scheme accommodates international through traffic, inter-island ferries, and other vessels whose routes frequently intersect, so traffic density alone cannot describe operational collision risk. This study aims to develop an auditable event-level framework that integrates Automatic Identification System data quality control, encounter reconstruction, closest-point-of-approach urgency, bidirectional ship-domain intrusion, exposure-adjusted comparison, and spatial risk mapping. AIS messages are cleaned and linked to verified vessel metadata, trajectories are reconstructed on a common time grid, and unique pairwise encounters are segmented before DCPA, TCPA, encounter geometry, and dynamic ship-domain status are calculated. One representative point per encounter is then used for temporal, vessel-class, and kernel-density analyses, with vessel-time exposure used as the spatial denominator. Because the original AIS and Vessel Traffic Service files were not available during this reconstruction, the workflow is demonstrated with a fixed-seed synthetic dataset. The prototype contains 2,135 encounter events; 384 events are classified as high CPA urgency, 412 contain a ship-domain breach, and 246 satisfy both conditions. The synthetic high-urgency rate is higher at night than during the day, ferry-involved encounters have the largest exposure-adjusted breach rate, and the northern precautionary zone has the highest adjusted critical-event intensity. The novelty is the transparent separation of encounter frequency, kinematic urgency, geometric intrusion, traffic exposure, and spatial concentration within one reproducible event master file. The framework is suitable for retrospective VTS calibration and safety evaluation, but every numerical result must be regenerated and validated with the original AIS and VTS records before it is interpreted as empirical evidence.

Keywords— AIS; collision risk; DCPA; kernel density estimation; Lombok Strait; ship domain; TCPA; traffic separation scheme.

[*]*Coressponding Author: nennybarombong@gmail.com*

I. INTRODUCTION

The Lombok Strait is a deep-water route connecting the Indian Ocean with the Indonesian archipelagic sea lanes and onward routes toward the western Pacific. The International Maritime Organization adopted a Traffic Separation Scheme (TSS) and associated routeing measures for the strait in 2019 [1]. The nearby Nusa Penida and Gili Matra areas were subsequently designated as a Particularly Sensitive Sea Area, which increases the consequence of navigational accidents near environmentally sensitive waters [2]. The corridor is therefore not only strategically important but also operationally complex: deep-draft merchant vessels move longitudinally through the TSS while ferries, local craft, fishing vessels, and service traffic may cross or operate near the traffic lanes.

Strategic models such as IWRAP estimate collision frequencies from route geometry, traffic flow, ship categories, and causation factors [3]. Such models are valuable for route planning and high-level safety assessment, including prior work in the Lombok Strait [31]. However, a high traffic count does not necessarily mean that vessels repeatedly approach unsafe separation. Conversely, a location with moderate traffic can generate short decision windows when crossing flows converge. AIS data provide the time-stamped positions, speeds, courses, identities, and selected dimensions needed to examine those interactions at encounter level [4].

The operational problem is that AIS-based risk maps can become misleading when four issues are not controlled. First, repeated messages from the same vessel pair may be counted as separate encounters and inflate event totals. Second, DCPA and TCPA describe projected relative motion but not whether one or both vessels enter a directional safety margin. Third, vessel-class percentages can mix unique vessels, pair involvement, and event contribution even though these denominators answer different questions. Fourth, an unadjusted kernel-density map can reproduce ordinary traffic concentration rather than collision-related intensity. These problems are particularly relevant in a TSS where through traffic and recurrent ferry crossings coexist.

Near-miss research has produced mature methods for detecting critical ship encounters from DCPA, TCPA, relative motion, avoidance behavior, and ship-domain violations [5]-[10]. Regional studies have also used kernel density, gridded risk surfaces, machine learning, and spatiotemporal prediction to locate and forecast collision-prone areas [11], [14]-[23]. Nevertheless, many applications emphasize one risk indicator or one output surface. Less attention is given to whether all tables, statistical models, intersections, and maps can be traced back to the same unique encounter event and reconciled with explicit denominators.

Nenny., Politeknik Pelayaran Barombong, Makassar, Indonesia, 90225, Indonesia. E-mail: nennybarombong@gmail.com

Adnan, Politeknik Pelayaran Barombong, Makassar, Indonesia, 90225, Indonesia. E-mail: adnan17.makassar@gmail.com

Joe Ronald K. Bokau, Politeknik Pelayaran Barombong, Makassar, Indonesia, 90225, Indonesia. Email: joeronald@poltekpelbarombong.ac.id

Muh. Arifin, Universitas Muhammadiyah Parepare, Parepare, 91112, Indonesia,. E-mail: arifin.abidin@gmai.com

The source version of this manuscript referred to the PARK model, but it did not provide the complete equation, coefficients, or local calibration needed for independent replication. PARK therefore remains part of the literature background [12], whereas the present reconstruction uses a fully specified CPA-based urgency index whose inputs are directly observable in AIS records. This choice does not claim that the proposed index is universally superior. It ensures that reviewers and VTS analysts can reproduce each event classification and test alternative thresholds.

The study contributes four linked innovations. It constructs one unique pairwise event before calculating risk, applies ship-domain status in both vessel directions, uses explicit exposure denominators for temporal, class, and spatial comparisons, and defines integrated critical events as the verifiable intersection of high CPA urgency and domain breach rather than as an opaque composite score. The approach preserves the individual risk dimensions so that the same final count cannot conceal different operational mechanisms.

The objective is to develop and demonstrate a reproducible AIS collision-risk mapping framework for the Lombok Strait TSS that links data cleaning, event reconstruction, CPA urgency, bidirectional ship-domain intrusion, exposure adjustment, and spatial prioritization. The analysis addresses four questions: (1) how can raw AIS reports be converted into unique and auditable encounter events; (2) how do CPA urgency and ship-domain intrusion differ and intersect; (3) how should temporal, vessel-class, and hotspot patterns be compared without denominator or exposure bias; and (4) how can the resulting outputs be implemented and validated within a VTS safety-learning process?.

II. LITERATURE REVIEW

A. AIS Quality Control and Encounter Reconstruction

AIS supports maritime surveillance because dynamic messages report position, speed, course, heading, and navigational status, while static messages provide identity and dimensional information [4]. The same data are affected by duplicate records, irregular reporting intervals, erroneous coordinates, identity conflicts, missing dimensions, and spoofed or manually entered attributes. These limitations matter because a small positional or temporal error can change DCPA, TCPA, encounter geometry, and domain status. Consequently, collision-risk analysis should report message cleaning, track segmentation, interpolation limits, and vessel-identity validation before presenting risk results.

Event reconstruction is equally important. Early and advanced near-miss methods showed that a candidate conflict should be understood as a developing interaction rather than as an isolated AIS timestamp [5], [6]. Review work on AIS-derived non-accident critical events has emphasized that detection rules, encounter duration, and threshold selection substantially affect the number of reported events [7]. The present study follows that logic by using entry and exit radii, a minimum duration, a merging gap, and sorted pair identifiers. This prevents A-B and B-A duplication and avoids counting every resampled timestamp as a separate event.

B. CPA Metrics and Encounter Urgency

DCPA and TCPA remain widely used because they provide an interpretable description of relative motion. DCPA estimates the minimum projected separation under a constant-velocity assumption, while TCPA estimates the time remaining to that position. Their limitations are also well established: a low DCPA with a long TCPA may not require immediate action, and a short TCPA with a comfortable DCPA may not indicate dangerous proximity. Fuzzy, velocity-obstacle, multivariate, and machine-learning methods have therefore been proposed to combine kinematic variables and contextual information [15], [24], [25], [28], [30], [33].

The present urgency index uses bounded DCPA and TCPA memberships and their geometric mean. This construction requires both spatial closeness and temporal immediacy to be present for a high score. It is deliberately simpler than a predictive neural network or an expert-weighted multicriteria model. Simplicity is useful here because the objective is retrospective auditability: every score can be recomputed directly from the event record and alternative threshold sets can be examined without retraining a model.

C. Ship Domains and Geometric Intrusion

A ship domain represents the directional space that a navigator generally seeks to keep free around a vessel. Reviews and comparative studies show that domain size and shape vary with vessel dimensions, speed, encounter orientation, waterway constraints, and navigator behavior [8]-[10]. Empirical AIS research has estimated domains from evasive maneuvers and surrounding traffic distributions [18], [19]. These studies demonstrate why one fixed circular buffer is inadequate for mixed traffic involving ferries, tankers, container ships, and bulk carriers.

Domain intrusion is related to, but not identical with, CPA urgency. A target may breach the domain of a large or fast vessel even when the reciprocal domain is not breached. Conversely, a low projected DCPA may occur before the vessels enter either domain. Calculating the domain in both directions therefore identifies unilateral and bilateral loss of geometric margin. The present framework also separates brief transient intrusions from sustained episodes so that a single noisy position is not treated as persistent risk.

D. Spatial Risk Mapping and Exposure Adjustment

Kernel Density Estimation converts discrete event locations into a continuous surface and is useful for visual prioritization [11], [36]. Yet the interpretation depends on what is being smoothed. A density of AIS messages describes reporting concentration; a density of encounter points describes interaction concentration; and a density weighted by urgency or intrusion describes a different risk dimension. Regional risk models increasingly combine gridding, domain methods, clustering, and spatiotemporal prediction [16], [21], [23], [26], [29], [30]. The broad literature therefore supports spatial analysis, but it also shows that bandwidth, grid resolution, edge effects, and threshold definitions can materially change a hotspot.

Exposure adjustment is necessary when the purpose is to compare areas rather than count activity. A busy lane may contain many events because many vessels pass through it, while a lower-volume crossing area may have a larger rate of critical events per unit of vessel-time. The present framework calculates separate surfaces for encounter frequency, CPA urgency, intrusion depth, and critical-event incidence, then divides the weighted event surface by a vessel-time exposure surface. This preserves the distinction between where traffic is concentrated and where a vessel operating in that area is relatively more likely to experience a critical interaction.

E. TSS-Specific Evidence and Synthesis

Studies of constrained straits and port waters show that crossing angle, route organization, vessel mix, and local environmental conditions influence collision risk [17], [27]-[32]. In the Lombok Strait, previous strategic analysis identified the importance of longitudinal international traffic, cross-strait ferry activity, and environmental consequences near Nusa Penida [31]. A TSS may reduce disorder in opposing through traffic, but it does not remove encounters created where local routes cross or merge with the scheme.

The literature therefore supports the components used in this study, but it does not eliminate the need for an integrated audit trail. The novelty lies in making each component answer a different question within one event master file: how often encounters occur, how urgently they converge, whether directional domains are entered, how much traffic is exposed, and where critical intersections concentrate. This structure also resolves the logical requirement that the number of events classified as both high urgency and domain breach cannot exceed either marginal total

III. METHOD

A. Study Design, Area, and Data Status

The planned empirical study is a retrospective observational analysis of AIS records within the Lombok Strait TSS, adjoining precautionary areas, ferry-crossing corridors, and an operational buffer from 13 to 19 February 2024. The unit of analysis is one unique unordered vessel-pair encounter event. Geographic coordinates use WGS 84, while distance calculations use UTM Zone 50S. The final empirical implementation requires authoritative lane boundaries, separation zones, precautionary areas, ferry routes, and coastline masks.

The current reconstruction is a methodological prototype. The original raw AIS and VTS records were not available during preparation of this revised document. A fixed-seed synthetic dataset was therefore generated to test the analytical sequence, mathematical constraints, table structure, figures, and journal layout. Synthetic results are reported only to demonstrate internal consistency and must not be represented as observed conditions in the Lombok Strait.

B. AIS Variables and Vessel-Metadata Validation

The minimum dynamic fields are Maritime Mobile Service Identity, timestamp, latitude, longitude, speed over ground, and course over ground. True heading, navigational status, rate of turn, vessel name, IMO number, call sign, ship type, length, beam, draught, and destination are retained when available. Dynamic and static reports are processed separately and linked through MMSI.

For each MMSI, the IMO number, vessel name, call sign, type code, length, and beam are checked for temporal consistency. Severe unresolved identity conflicts are excluded. AIS type codes are not treated as sufficient evidence for operational class: cargo codes cannot reliably distinguish bulk carriers from container ships, and passenger codes do not automatically establish a scheduled ferry service. Final classes should be assigned from registry information, VTS records, and validated route behavior.

C. Cleaning and Trajectory Reconstruction

Records are removed when timestamps are missing or duplicated, coordinates fall outside valid ranges, identity conflicts remain unresolved, or implied displacement speeds are physically implausible. Positions are clipped to the study polygon and operational buffer. A new trajectory begins when the reporting gap exceeds 10 min, when a vessel leaves and later re-enters the area, or when a discontinuity cannot be reconciled.

A valid trajectory contains at least five reports and spans at least 2 min. Trajectories are resampled to a common 30-s grid. Linear interpolation is allowed only for internal gaps of 120 s or less. The primary analysis does not apply Kalman smoothing because excessive smoothing can shift the timing or location of a closest approach; alternative smoothing may be evaluated as a sensitivity scenario.

D. Pairwise Encounter Segmentation and Geometry

At each synchronized timestamp, an unordered pair is created when both vessels are moving and their separation is 5 nautical miles or less. Consecutive observations are combined into one event using a 5-nautical-mile entry radius, a 6-nautical-mile exit radius, a minimum duration of 60 s, and a fragment-merging gap of 120 s. A sorted pair key prevents duplicate A-B and B-A events. The event start, end, duration, minimum separation, and representative time are retained.

Encounter geometry is assigned during the initial stable approach phase. A head-on event requires nearly reciprocal courses and reciprocal forward-sector bearings. Overtaking requires approximately parallel courses, an aft-sector target position, and a positive speed advantage for the overtaking vessel. Other stable converging geometries are classified as crossing in accordance with the operational interpretation of COLREG encounter situations [35]. Parallel, diverging, and uncertain candidates remain available for quality review rather than being forced into one of the three principal classes.

E. CPA-Based Urgency Index

SOG and COG are converted to eastward and northward velocity components. Let r be the relative position vector from vessel 1 to vessel 2 and u the relative velocity vector. Under a short-horizon constant-velocity assumption, TCPA and DCPA are calculated as follows:

$$TCPA = -(r \cdot u) / (u \cdot u) \quad (1)$$

$$DCPA = ||r + u \times TCPA|| \quad (2)$$

Negative TCPA indicates that the projected closest approach has passed. Calculations with negligible relative speed are excluded. Prospective urgency is evaluated only for converging observations with TCPA between 0 and 30 min. The DCPA membership equals 1.0 at or below 0.5 nautical miles, decreases linearly to 0 at 1.5 nautical miles, and is 0 beyond that distance. The TCPA membership equals 1.0 between 0 and 5 min, decreases linearly to 0 at 30 min, and is 0 outside the prospective window. The point-level urgency is:

$$R\_CPA = sqrt(mu\_D \times mu\_T) \quad (3)$$

The event score is the maximum point-level value during the stable approach. High urgency is defined as R_CPA at least 0.67, moderate urgency as 0.33-0.66, and low urgency as less than 0.33. These thresholds are transparent starting values and require calibration against observed VTS interventions, expert review, and near-miss records.

F. Bidirectional Ship-Domain Analysis

Each vessel is assigned a speed- and dimension-adjusted four-quadrant elliptical domain aligned with its heading. The prototype radii are R_F = 4L + 60V forward, R_A = 1.5L + 30V aft, and R_S = R_P = 3B + 30V laterally, where L and B are length and beam in metres and V is speed in metres per second. Static and empirically fitted domains are included in sensitivity analysis [8]-[10], [18], [19].

The target position is transformed into the own-ship coordinate system. The longitudinal radius R_L is selected from the forward or aft value and the transverse radius R_T from the starboard or port value. The normalized domain value is:

$$Q = (x\_long / R\_L)^2 + (y\_lat / R\_T)^2 \quad (4)$$

A breach occurs when Q is at most 1. Status is calculated from vessel 1 toward vessel 2 and again from vessel 2 toward vessel 1. Each observation is therefore classified as no breach, unilateral breach, or bilateral breach. Intrusion depth is max(0, 1 - sqrt(Q)). Consecutive breach observations are grouped into episodes; episodes shorter than 60 s are classified as transient.

G. Temporal, Vessel-Class, and Statistical Analysis

Each event is assigned to day, civil twilight, nautical twilight, or night from local solar elevation at the representative event time in Central Indonesian Time. The primary day-night comparison combines twilight with daytime or excludes it according to a prespecified sensitivity analysis. High-urgency, breach, and critical-event rates use eligible encounter events as denominators.

Vessel-class results distinguish three quantities. Unique-vessel composition describes the registry. Involvement rates use the number of eligible encounters containing a class as the denominator and may overlap because a pair can contain two different classes. Contribution percentages describe the share of all outcome events involving a class and should not be interpreted as risk without exposure adjustment. Pair-type comparisons are used for operational combinations such as ferry-tanker and ferry-container encounters.

For empirical inference, generalized estimating equations or mixed-effects logistic models should account for repeated involvement of vessel pairs and observation days. Prespecified covariates include night period, encounter geometry, ferry involvement, tanker involvement, vessel-size combination, and selected interaction terms. Odds ratios, 95% confidence intervals, and p-values must be reported together. Prototype odds ratios are descriptive demonstrations and are not evidence about the actual strait.

H. Exposure-Adjusted Spatial Analysis

One representative location is retained per event, selected at maximum CPA urgency or, for a domain-only event, at maximum intrusion depth. Gaussian KDE is calculated separately for event frequency, urgency weighted by R_CPA, intrusion weighted by maximum depth, and critical events defined by the high-urgency-and-breach intersection. A vessel-time exposure surface is produced from the resampled trajectories using the same projection and grid.

For each outcome, adjusted intensity is the weighted event KDE divided by the exposure surface plus a small stability constant. Hotspots are contiguous grid cells above the 90th percentile of the adjusted critical-event surface. The empirical report must state the coordinate system, bandwidth, grid resolution, exposure unit, edge correction, percentile threshold, and minimum polygon area. Bandwidths of 0.5 and 1.5 km, alternative thresholds, and leave-one-day-out maps are used to evaluate stability.

I. Integrity and Reproducibility Controls

All output tables and figures are generated from one encounter master file. The integrated critical group is defined as high CPA urgency AND any domain breach, so its count cannot exceed the high-urgency total or the breach total. Automated checks reconcile geometry totals, urgency totals, breach totals, period totals, zone totals, and their intersections. The analysis configuration, data dictionary, random seed for prototype generation, and code version are retained for audit.

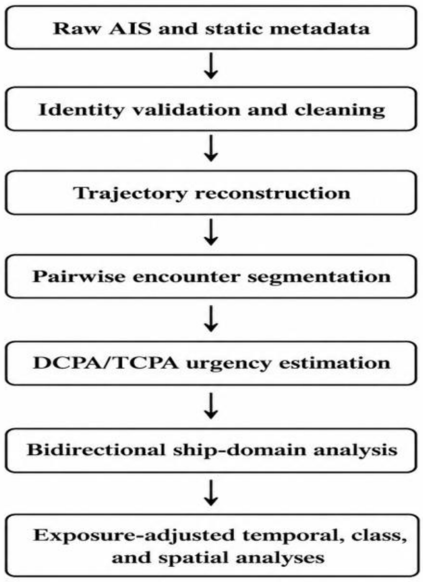

Figure 1. Auditable analytical workflow from raw AIS records to exposure-adjusted risk outputs

IV. RESULTS AND DISCUSSION

A. Data Flow and Vessel Composition

The fixed-seed prototype begins with 1,286,430 AIS messages. After timestamp, coordinate, duplicate, identity, and kinematic checks, 1,147,884 messages remain, corresponding to 89.2% message-level retention. The cleaned records form 6,734 initial trajectory segments; 5,982 satisfy the trajectory criteria. Pairwise screening creates 2,560 candidate episodes and 2,135 significant encounter events. Reporting these stages separately prevents message retention, trajectory retention, and encounter retention from being treated as the same quantity.

TABLE 1.
DATA-PROCESSING FLOW

Stage	Count	Retention (%)
Raw messages	1,286,430	100.0
Valid time and position	1,239,816	96.4
Deduplicated	1,201,442	93.4
Valid identity and kinematics	1,147,884	89.2
Initial trajectories	6,734	-
Valid trajectories	5,982	88.8
Candidate episodes	2,560	-
Significant encounters	2,135	83.4

The prototype registry contains 312 unique vessels: 81 tankers, 69 bulk carriers, 59 container ships, 44 ferries, and 59 other vessels. These percentages describe unique vessels only. They do not indicate how often each class transmitted, how long it remained in the area, or how many encounters it experienced. The distinction is important because ferries can represent a smaller share of unique vessels while generating repeated exposure through scheduled crossings.

B. Encounter Geometry and CPA Urgency

Crossing situations account for 896 events (42.0%), overtaking for 726 (34.0%), and head-on for 513 (24.0%). This distribution is not an empirical statement about ferry operations, but it demonstrates how event segmentation avoids the inflation that would occur if every synchronized observation were counted. The predominance of crossing geometry is operationally plausible in a corridor where local routes intersect longitudinal traffic, and similar research shows that crossing angle and navigational context affect regional risk estimates [32].

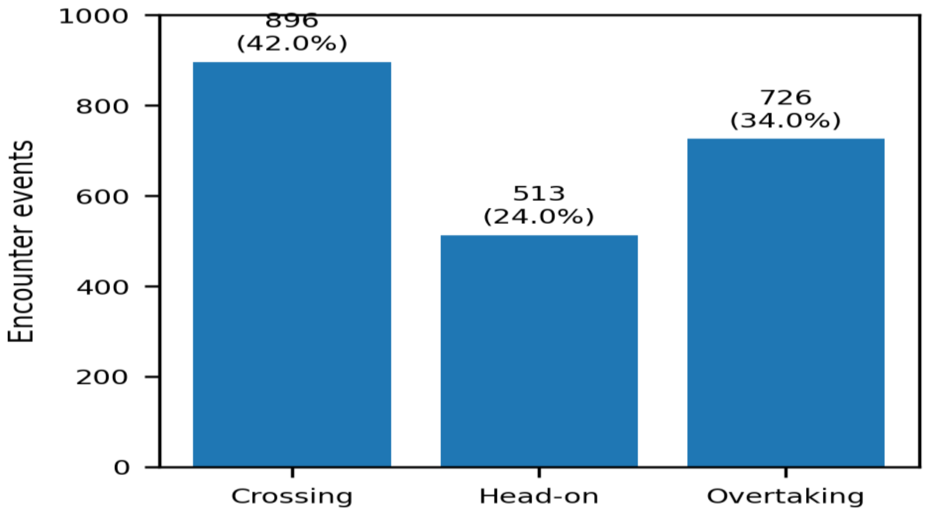

Figure 2. Distribution of encounter geometry in the fixed-seed prototype.

TABLE 2.
CPA URGENCY BY ENCOUNTER GEOMETRY

Geometry	Events	High	High (%)
Crossing	896	242	27.0
Head-on	513	91	17.7
Overtaking	726	51	7.0

The CPA index classifies 384 events (18.0%) as high urgency, 940 (44.0%) as moderate, and 811 (38.0%) as low. The high-urgency rate is 27.0% for crossing events, 17.7% for head-on events, and 7.0% for overtaking events. Counts alone would obscure this difference because overtaking events are numerous but have a comparatively low high-urgency rate. This supports geometry-specific reporting and is consistent with methods that incorporate crossing angle, relative motion, and waterway context rather than applying a single proximity threshold.

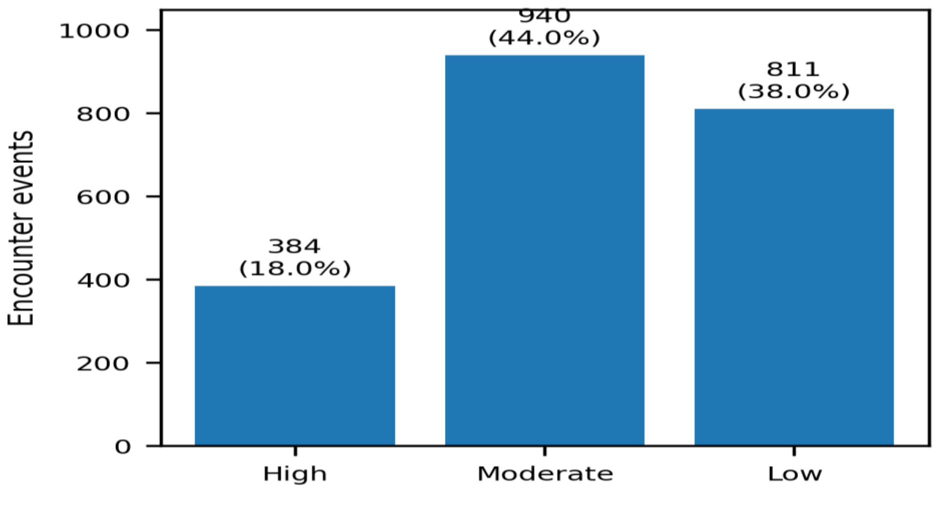

Figure 3. CPA-urgency categories at the unique encounter-event level.

The CPA index should not be interpreted as a collision probability. It is an urgency indicator under a constant-velocity projection. A high value means that a close projected approach and a short time window occur together. It does not show whether either navigator has detected the situation, whether an avoidance maneuver is already underway, or whether current and wind will change the projected motion. Avoidance-behavior methods and velocity-obstacle models could be added as validation layers rather than substituted without comparison.

C. Ship-Domain Intrusion and Integrated Critical Events

A ship-domain breach occurs in 412 of the 2,135 events (19.3%). Sixty-three events contain only a transient breach, 253 contain a sustained unilateral breach, and 96 contain a sustained bilateral breach. The unilateral category is substantively important because mixed-size or mixed-speed pairs need not experience reciprocal loss of domain margin. Bidirectional calculation therefore provides more information than a single symmetric buffer.

The critical integrated group contains 246 events that are both high CPA urgency and domain breach. The value is lower than the high-urgency total of 384 and the breach total of 412, satisfying the intersection constraint. This correction is more than an arithmetic detail. It preserves two distinct safety meanings: CPA urgency measures the projected time-distance combination, while domain breach measures penetration of a vessel-specific geometric margin. Events can satisfy one condition without satisfying the other, and VTS review should examine those discordant groups rather than compress them into one score.

TABLE 3.
SHIP-DOMAIN STATUS

Domain status	Events	Percent
No breach	1,723	80.7
Transient breach	63	3.0
Sustained unilateral	253	11.9
Sustained bilateral	96	4.5

Recent domain research has emphasized that domain parameters depend on vessel characteristics and observed maneuvering behavior. The prototype uses an explicit dynamic ellipse because it can be reproduced, not because the coefficients are assumed to be locally optimal. The empirical study should compare the chosen specification with static, empirical, and class-specific domains and should report agreement, false alarms, missed expert-labelled events, and warning lead time.

D. Temporal Differences

Daytime contains 1,153 prototype encounters and nighttime contains 982. The high-urgency rate is 13.0% during daytime and 23.8% at night, producing an unadjusted odds ratio of 2.09 (95% CI 1.67-2.62). Domain-breach rates are 15.0% and 24.3%, respectively, with an odds ratio of 1.82 (95% CI 1.47-2.27). The critical-event rate increases from 7.4% to 16.4%. In the illustrative adjusted models, the nighttime associations remain positive after geometry and selected class involvement are included.

TABLE 4.
DAY-NIGHT COMPARISON

Outcome	**Day (%)**	**Night (%)**	**OR**	**95% CI**
High CPA urgency	13.0	23.8	2.09	1.67-2.62
Domain breach	15.0	24.3	1.82	1.47-2.27
Critical event	7.4	16.4	2.46	1.87-3.25

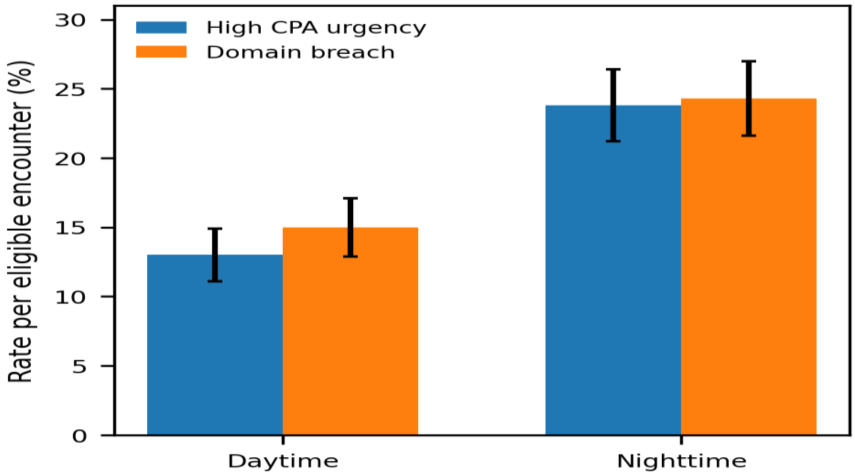

Figure 4. Prototype high-urgency and domain-breach rates by period; error bars are approximate 95% confidence intervals.

The result format is useful, but the synthetic difference cannot support a causal claim that darkness increases collision risk. Night is a proxy that can coincide with visibility, fatigue, ferry schedules, traffic composition, current, weather, and VTS staffing. Research combining AIS with hydrometeorological data shows that environmental conditions can alter the interpretation of encounter risk [34]. The empirical analysis should therefore integrate weather, visibility, current, and intervention records where their timing and quality are sufficient. At minimum, the discussion should use associative language and report how the estimate changes after those covariates are added.

E. Vessel-Class and Pair-Type Patterns

Ferry-involved encounters have the highest prototype high-urgency rate (26.4%) and domain-breach rate (27.2%). Container ships and tankers have similar breach rates, while bulk carriers and other vessels have lower rates. The eligible counts are involvement denominators, so they overlap across classes. This is the correct structure for asking how often an encounter involving a given class contains an outcome. It is different from asking what percentage of all breaches involve that class.

TABLE 5.
EXPOSURE-ADJUSTED VESSEL-CLASS RATES

Class	Eligible	High (%)	Breach (%)
Ferry	784	26.4	27.2
Tanker	835	19.0	19.2
Container ship	851	17.3	19.3
Bulk carrier	963	15.6	16.4
Other	411	13.4	13.9

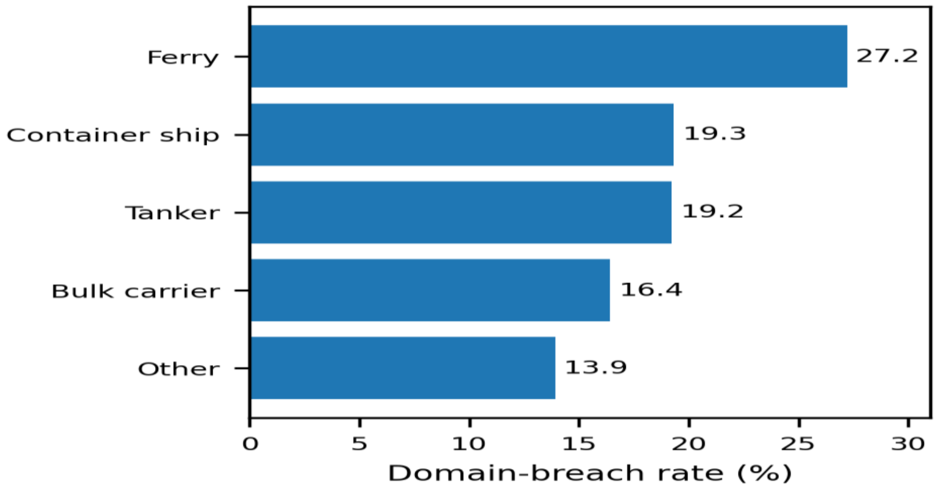

Figure 5. Prototype domain-breach rate by vessel-class involvement

.

Pair-type analysis further separates ferry-tanker, ferry-bulk-carrier, ferry-container-ship, and ferry-ferry events. In the prototype, ferry-container and ferry-bulk pairs have breach rates near 30%, while the ferry-tanker high-urgency rate is 29.9%. These comparisons are operationally more useful than a broad statement that ferries contribute many events, because scheduled repetition and route geometry can create high exposure. The empirical interpretation should compare pair-specific rates, encounter angles, speed differences, and the side of domain intrusion.

The result illustrates the intended contribution to TSS evaluation. Longitudinal traffic may be orderly within the lane while recurrent crossings create a greater proportion of urgent interactions. A VTS response should therefore not be based solely on vessel type. It should consider route, pair composition, encounter geometry, and time window. Any ferry-specific threshold also requires validation to avoid penalizing predictable crossings that are safely coordinated.

F. Spatial Risk and Hotspot Interpretation

The synthetic coordinates assign 994 encounters to the central TSS corridor, 815 to the northern precautionary zone, and 326 to the southern approach. Raw encounter count is highest in the central corridor. The northern zone nevertheless has the highest high-urgency rate (22.2%), breach rate (24.0%), and exposure-adjusted critical-event intensity. This contrast demonstrates why an encounter-density map and a risk-intensity map should not be described as the same output.

TABLE 6.
ZONE CHARACTERISTICS

Zone	Events	High (%)	Breach (%)
Central TSS	994	18.8	19.5
Northern precautionary zone	815	22.2	24.0
Southern approach	326	4.9	6.7

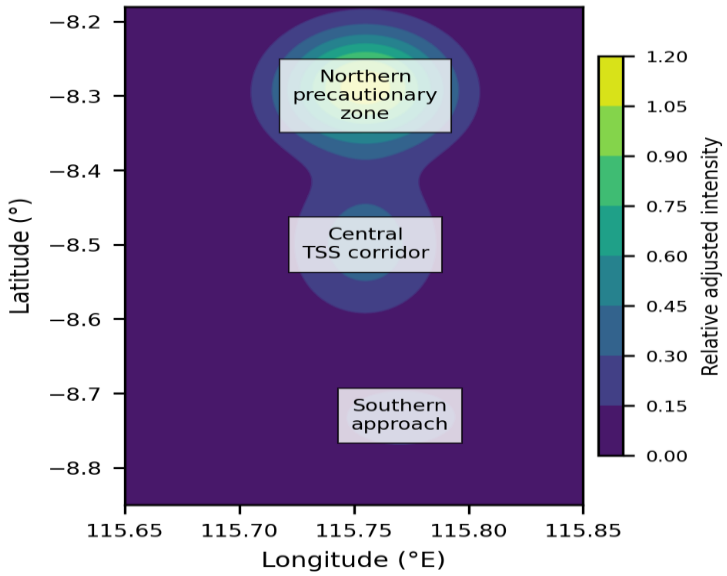

Figure 6. Schematic exposure-adjusted critical-event surface from synthetic coordinates; it is not an authoritative navigational map

.

KDE is a prioritization tool rather than proof of collision probability. The apparent position and extent of a hotspot depend on bandwidth, projection, grid size, boundary treatment, event weighting, and exposure definition. The term persistent should not be used for a seven-day observation period unless the polygon remains stable across days, parameter settings, seasons, and an independent validation period. For operational use, a hotspot should be accompanied by event samples, trajectory replays, and the numerator and exposure values that produced the surface.

The exposure-adjusted map is the spatial novelty of the framework. Existing regional models demonstrate the value of gridded and spatiotemporal risk analysis The present approach adds denominator traceability: the analyst can inspect whether a high cell results from many ordinary encounters, a smaller number of severe encounters, low vessel-time exposure, or a combination of those factors. That distinction determines whether VTS action should focus on traffic organization, warning timing, route design, or targeted operator review.

G. Sensitivity and Methodological Contribution

The prototype high-urgency count varies from 326 to 447 under alternative CPA specifications. Domain-breach counts vary from 356 under a static domain to 468 when the broader screening specification changes event eligibility. Hotspot overlap ranges from 0.86 to 0.96. These results show that broad spatial patterns can remain recognizable even when event totals are threshold-sensitive. They also show why one preferred configuration should not be presented without uncertainty or robustness checks.

TABLE 7.
SELECTED SENSITIVITY SCENARIOS

Scenario	High	Breach	Hotspot overlap
TCPA window: 20 min	339	352	0.89
TCPA window: 45 min	421	446	0.95
DCPA upper bound: 1.0 NM	326	361	0.86
DCPA upper bound: 2.0 NM	447	468	0.93
Static ellipse	384	356	0.86
KDE bandwidth: 0.5 km	384	412	0.92
KDE bandwidth: 1.5 km	384	412	0.96

The main methodological contribution is not a universal collision-risk score. It is an auditable integration that retains the variables needed to reproduce every event: original message identifiers, pair key, geometry, DCPA, TCPA, urgency membership, domain direction, intrusion depth, vessel classes, time category, exposure denominator, representative point, and sensitivity label. This event-level traceability is complementary to advanced predictive models [33], [34]. A complex model may improve discrimination, but it should still preserve enough provenance for an operator or reviewer to understand why a particular encounter was prioritized.

H. VTS Implementation Roadmap

Implementation should proceed in four governed stages. First, historical AIS tracks should be replayed and a stratified sample of high-urgency, breach, critical, and low-risk encounters should be reviewed by experienced VTS operators. Second, DCPA, TCPA, domain, and spatial thresholds should be calibrated against VTS near-miss logs and intervention records. Precision, sensitivity, false-alarm rate, missed-event rate, and alert lead time should be reported together. Third, the model should run in shadow mode without issuing operational instructions, while operators record agreement and disagreement using standardized reason codes. Fourth, controlled decision support may be considered only after performance, usability, cybersecurity, and governance requirements are satisfied.

TABLE 8.
PROTOTYPE VTS IMPLEMENTATION ROADMAP

Stage	Primary action	Required output
Retrospective replay	Manual event review	Agreement and error log
Calibration	Compare VTS logs and thresholds	Sensitivity, precision, and lead time
Shadow mode	Operator review only	Usability and nuisance-alert evidence
Controlled support	Governed attention cue	Audited operational evaluation

The system should prioritize attention rather than replace COLREG judgment, the bridge team, or VTS authority. Each alert must remain traceable to the underlying AIS observations and configuration. Access control, audit logs, data-retention rules, spoofing checks, and procedures for erroneous static data are essential. Environmental information, ferry schedules, navigational warnings, and traffic-management rules should be integrated only after their temporal resolution and reliability have been verified.

I. Limitations and Empirical Replacement Requirements

The principal limitation is that all numerical results in this version are synthetic. The prototype contains no original AIS messages, verified MMSI-IMO linkage, observed trajectories, authoritative TSS polygon, environmental measurements, or VTS near-miss validation. The seven-day design will also limit seasonal inference even after the raw data are analyzed. Consequently, the manuscript can demonstrate a method and a reporting structure, but it cannot support claims about the actual frequency, time pattern, vessel class, or location of collision risk in the Lombok Strait.

Before empirical submission, every number, model, table, confidence interval, coordinate, map, and conclusion must be regenerated from the original records. The affiliations and corresponding author must be confirmed, data-access and ethics statements completed, and the manuscript metadata made identical to the author list in the document. An independent audit should verify that the abstract, results, discussion, and conclusion use the same event master file and the same denominators.

V. CONCLUSION

This study set out to develop an auditable AIS collision-risk mapping framework for the Lombok Strait TSS. The objective is met methodologically by linking AIS quality control, trajectory reconstruction, unique pairwise event segmentation, CPA-based urgency, bidirectional ship-domain intrusion, exposure-adjusted temporal and vessel-class comparison, and adjusted KDE mapping within one reproducible event master file.

The fixed-seed demonstration produces 2,135 encounter events, including 384 high-urgency events, 412 domain breaches, and 246 events at their valid intersection. It also illustrates higher nighttime outcome rates, higher ferry-involved breach rates, and an adjusted northern-zone hotspot. These values confirm arithmetic consistency and show how the framework distinguishes frequency, urgency, intrusion, exposure, and spatial concentration. They are not empirical evidence about the Lombok Strait.

The next step is to execute the documented workflow on the original AIS and VTS data, validate vessel identities and encounter labels, calibrate thresholds with operator-reviewed events, integrate reliable environmental covariates, and regenerate all outputs. Only after that process should the results be used to support VTS evaluation, traffic-management decisions, or claims about collision risk in the Lombok Strait TSS.

ACKNOWLEDGEMENTS

The authors would like to express their gratitude to Politeknik Ilmu Pelayaran Makassar and Universitas Muhammadiyah Parepare for academic support in the development of this article. Appreciation is also extended to maritime practitioners and safety stakeholders whose perspectives have contributed to the conceptual strengthening of this study.

REFERENCES

[1] A. Alvarez, F. Pineda, and M. Martínez, "Machinery space fire casualty analysis in commercial ships," *WMU Journal of Maritime Affairs*, vol. 18, no. 4, pp. 567–584, 2019.
[2] H. Zhang, C. Li, N. Zhao, B. Q. Chen, H. Ren, and J. Kang, "Fire risk assessment in engine rooms considering the fire-induced domino effects," *Journal of Marine Science and Engineering*, vol. 10, no. 11, p. 1685, 2022, doi: 10.3390/jmse10111685.
[3] C. Li, H. Zhang, Y. Zhang, and J. Kang, "Fire risk assessment of a ship's power system under the conditions of an engine room fire," *Journal of Marine Science and Engineering*, vol. 10, no. 11, p. 1658, 2022, doi: 10.3390/jmse10111658.
[4] J. Zhu, J. Zhang, Y. Wang, Y. Ge, Z. Zhang, and S. Zhang, "Fire detection in ship engine rooms based on deep learning," *Sensors*, vol. 23, no. 14, p. 6552, 2023, doi: 10.3390/s23146552.
[5] H. Kim, J. Lee, and S. Park, "Smoke detection of marine engine room based on sensor fusion," *Journal of Marine Science and Engineering*, vol. 9, no. 8, p. 876, 2021.
[6] F. Khan, M. Yang, and R. Abbassi, "Risk evolution from causes to consequences of engine room fire hazards," *Safety Science*, vol. 115, pp. 191–202, 2019.
[7] J. Chen, Y. Zhang, and S. Wang, "Fire risk assessment of ship engine rooms based on fuzzy event tree analysis," *Journal of Marine Science and Engineering*, vol. 9, no. 4, p. 412, 2021.

[8] Y. Li, G. Chen, and L. Zhang, "A review of ventilation systems and fire incidents on ships," *Mathematical Modelling of Engineering Problems*, vol. 7, no. 4, pp. 615–623, 2020.

[9] Z. Wang, Y. Liu, and J. Chen, "Effects of ventilation system design on flame behavior and smoke characteristics for mitigating marine engine room fire hazards," *Ocean Engineering*, 2023.

[10] J. Li, H. Wang, and Q. Zhang, "Large-scale experimental investigation of the effect of mechanical ventilation on engine room fire behavior," *Fire Technology*, 2022.

[11] X. Liu, Y. Wang, and Z. Zhao, "Fire risk assessment in ship engine rooms considering system interaction," *Journal of Marine Science and Engineering*, vol. 10, no. 2, p. 245, 2022.

[12] International Maritime Organization, *International Convention for the Safety of Life at Sea (SOLAS), 1974, as amended*. London, U.K.: IMO, 2010.

[13] International Maritime Organization, *International Convention on Standards of Training, Certification and Watchkeeping for Seafarers (STCW), 1978, as amended*. London, U.K.: IMO, 2017.

[14] International Maritime Organization, *Model Course 7.04: Officer in Charge of an Engineering Watch*. London, U.K.: IMO, 2015.

[15] U. Uğurlu, E. Yıldız, and O. Başar, "A hybrid model for human-factor analysis of engine-room fires on ships: HFACS-PVFFTA," *Ocean Engineering*, vol. 217, 2020.

[16] Y. Sun, J. Zhang, and G. Chen, "Human factors analysis of engine room fire accidents using HFACS," *Ocean Engineering*, vol. 215, 2020.

[17] M. Rahimi, R. Abbassi, and V. Garaniya, "Integrated fire safety framework for ship machinery spaces," *Journal of Marine Science and Engineering*, vol. 10, no. 6, p. 744, 2022.

[18] J. Wang, Z. Yang, and K. Li, "Fire risk assessment of ship power systems under engine room fire conditions," *Journal of Marine Science and Engineering*, vol. 8, no. 11, p. 879, 2020.

[19] R. Oliveira, J. Silva, and P. Costa, "Fire detection sensors for marine engine rooms: A review," *Sensors*, vol. 21, no. 15, p. 5021, 2021.

[20] J. Park, D. Kim, and S. Lee, "Experimental study on water mist fire suppression system in ship engine rooms," *Fire Technology*, vol. 57, no. 6, pp. 2815–2836, 2021.

[21] G. Chen, Y. Li, and H. Zhang, "Evaluation of CO_2 fire extinguishing systems effectiveness in ship engine rooms," *Journal of Marine Science and Engineering*, vol. 9, no. 7, p. 702, 2021.

[22] Y. Zhao, X. Wang, and Q. Liu, "Fire safety barrier analysis in ship machinery spaces using bow-tie method," *Journal of Marine Science and Engineering*, vol. 10, no. 9, p. 1216, 2022.

[23] X. Bao, Y. Wang, and Z. Li, "Causal chain analysis of ship fire accidents using Bayesian network and safety barrier theory," *Reliability Engineering & System Safety*, 2023.

[24] L. Chen, P. Zhang, and H. Wang, "Comprehensive evaluation of marine ship fires risk based on fuzzy broad learning system," *Journal of Marine Science and Engineering*, vol. 11, no. 7, p. 1276, 2023, doi: 10.3390/jmse11071276.

[25] A. G. Kim, S. Lee, and J. Park, "Advancing maritime safety: Early detection of ship fires through intelligent vision-based systems," *Fire*, vol. 7, no. 3, p. 84, 2024, doi: 10.3390/fire7030084.

[26] X. Bai, Z. Tao, X. Xu, C. Zhou, and Y. Wang, "A review of ship fire detection technologies in maritime transportation," *Ocean Engineering*, vol. 346, p. 123989, 2026, doi: 10.1016/j.oceaneng.2025.123989.

[27] A. Komianos, B. Navas de Maya, G. Psarros, O. C. Astrup, G. Theotokatos, E. Boulougouris, and D. Vassalos, "Fire prevention and mitigation measures onboard large passenger ships," in *Proc. 1st International Conference on the Stability and Safety of Ships and Ocean Vehicles*, Glasgow, U.K., 2021.

[28] Gard, "Fire safety onboard ships: A continuous cause for concern," *Gard Insight*, 2022.

[29] C. Sakar, M. Buber, B. Koseoglu, and A. C. Toz, "Risk analysis for confined space accidents onboard ship using fuzzy bow-tie methodology," *Ocean Engineering*, vol. 263, p. 112386, 2022, doi: 10.1016/j.oceaneng.2022.112386.

[30] Y. Li, H. Zhang, and C. Wang, "An integrated risk assessment framework for fire accidents on passenger ships," *Ocean Engineering*, 2025.

[31] R. J. Torraco, "Writing integrative literature reviews: Guidelines and examples," *Human Resource Development Review*, vol. 4, no. 3, pp. 356–367, 2005.

[32] H. Snyder, "Literature review as a research methodology: An overview and guidelines," *Journal of Business Research*, vol. 104, pp. 333–339, 2019, doi: 10.1016/j.jbusres.2019.07.039.

[33] R. Whittemore and K. Knafl, "The integrative review: Updated methodology," *Journal of Advanced Nursing*, vol. 52, no. 5, pp. 546–553, 2005.

[34] J. Reason, *Managing the Risks of Organizational Accidents*. Aldershot, U.K.: Ashgate, 1997.

[35] M. J. Page *et al*., "The PRISMA 2020 statement: An updated guideline for reporting systematic reviews," *BMJ*, vol. 372, p. n71, 2021.

[21] G. Chen, Y. Li, and H. Zhang, "Evaluation of CO_2 fire extinguishing systems effectiveness in ship engine rooms," *Journal of Marine Science and Engineering*, vol. 9, no. 7, p. 702, 2021.

[22] Y. Zhao, X. Wang, and Q. Liu, "Fire safety barrier analysis in ship machinery spaces using bow-tie method," *Journal of Marine Science and Engineering*, vol. 10, no. 9, p. 1216, 2022.

[23] X. Bao, Y. Wang, and Z. Li, "Causal chain analysis of ship fire accidents using Bayesian network and safety barrier theory," *Reliability Engineering & System Safety*, 2023.

[24] L. Chen, P. Zhang, and H. Wang, "Comprehensive evaluation of marine ship fires risk based on fuzzy broad learning system," *Journal of Marine Science and Engineering*, vol. 11, no. 7, p. 1276, 2023, doi: 10.3390/jmse11071276.

[25] A. G. Kim, S. Lee, and J. Park, "Advancing maritime safety: Early detection of ship fires through intelligent vision-based systems," *Fire*, vol. 7, no. 3, p. 84, 2024, doi: 10.3390/fire7030084.

[26] X. Bai, Z. Tao, X. Xu, C. Zhou, and Y. Wang, "A review of ship fire detection technologies in maritime transportation," *Ocean Engineering*, vol. 346, p. 123989, 2026, doi: 10.1016/j.oceaneng.2025.123989.

[27] A. Komianos, B. Navas de Maya, G. Psarros, O. C. Astrup, G. Theotokatos, E. Boulougouris, and D. Vassalos, "Fire prevention and mitigation measures onboard large passenger ships," in *Proc. 1st International Conference on the Stability and Safety of Ships and Ocean Vehicles*, Glasgow, U.K., 2021.

[28] Gard, "Fire safety onboard ships: A continuous cause for concern," *Gard Insight*, 2022.

[29] C. Sakar, M. Buber, B. Koseoglu, and A. C. Toz, "Risk analysis for confined space accidents onboard ship using fuzzy bow-tie methodology," *Ocean Engineering*, vol. 263, p. 112386, 2022, doi: 10.1016/j.oceaneng.2022.112386.

[30] Y. Li, H. Zhang, and C. Wang, "An integrated risk assessment framework for fire accidents on passenger ships," *Ocean Engineering*, 2025.

[31] R. J. Torraco, "Writing integrative literature reviews: Guidelines and examples," *Human Resource Development Review*, vol. 4, no. 3, pp. 356–367, 2005.

[32] H. Snyder, "Literature review as a research methodology: An overview and guidelines," *Journal of Business Research*, vol. 104, pp. 333–339, 2019, doi: 10.1016/j.jbusres.2019.07.039.

[33] R. Whittemore and K. Knafl, "The integrative review: Updated methodology," *Journal of Advanced Nursing*, vol. 52, no. 5, pp. 546–553, 2005.

[34] J. Reason, *Managing the Risks of Organizational Accidents*. Aldershot, U.K.: Ashgate, 1997.

[35] M. J. Page *et al*., "The PRISMA 2020 statement: An updated guideline for reporting systematic reviews," *BMJ*, vol. 372, p. n71, 2021.